Environmental Pollution 339 (2023) 122658

Contents lists available at ScienceDirect

Environmental Pollution

journal homepage: www.elsevier.com/locate/envpol

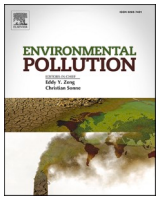

Characterisation of former manufactured gas plant soils using parent and alkylated polycyclic aromatic hydrocarbons and Rock-Eval(6) pyrolysis☆

Alison M. Williams-Clayson [a,b], Christopher H. Vane [a], Matthew D. Jones [b], Russell Thomas [c], Alexander W. Kim [a], Christopher Taylor [d], Darren J. Beriro [a,*]

[a] British Geological Survey, Keyworth, Nottinghamshire, UK
[b] University of Nottingham, Nottingham, UK
[c] WSP UK, Bristol, UK
[d] National Grid, Warwick, UK

ARTICLE INFO

Keywords:
Gasworks
Contamination
PAH
GC-MS/MS
Rock-Eval

ABSTRACT

Soils sampled from 10 former manufactured gas plants (MGP) in the UK were investigated using gas chromatography mass spectrometry (GC-MS/MS) and Rock-Eval (6) Pyrolysis (RE). RE is a screening tool used to characterise bulk organic matter in soils via the release of carbon compounds during pyrolysis and oxidation. Both the distributions and concentrations of 30 parent and 21 alkylated polycyclic aromatic hydrocarbons (PAHs) and the parameters of RE were analysed to establish relationships between soils and the MGP processes history. Principal component analysis (PCA) using the PAHs distributions and RE parameters can assist with differentiating between MGP processes. MGP processes utilizing oil provided the clearest results, attributed to petrogenic signatures with high proportions of low molecular weight PAHs. Processes using lower temperature processes were distinguished by higher proportions of high molecular weight PAHs. RE parameters alone were unable to distinguish MGP processes but showed potential in estimating the lability and thus the amount of PAH that could be released from soils. This research provides new insights that may be useful in understanding and characterising the risks posed to human health from PAHs in soils.

1. Introduction

Polycyclic aromatic hydrocarbons (PAHs) are a class of organic compounds and are a concern to human health due to their toxicity, with several PAHs classified as being mutagenic and carcinogenic (INTERNATIONAL AGENCY FOR RESEARCH ON CANCER, 2010). In the environment, PAHs can be persistent in soil as complex mixtures, comprising of parent PAHs (basic fused aromatic ring structure), alkylated PAHs (additional hydrocarbon chain attached), or heteroatom containing PAHs (containing non carbon/hydrogen elements). The most studied PAH group is the 16 U.S Environmental Protection Agency PAHs (EPA16) which comprise solely of parent PAHs: naphthalene (Nap), acenaphthylene (Acy), acenaphthene (Ace), fluorene (Flu), phenanthrene (Phen), anthracene (An), fluoranthene (Fla), pyrene (Pyr), benzo[*a*]anthracene (BaA), chrysene (Chry), benzo[*b*]fluoranthene (BbF), benzo[*k*]fluoranthene (BkF), benzo[*a*]pyrene (BaP), indeno[1,2,3-*cd*]pyrene (IcdP), dibenz[*a,h*]anthracene (DahA), and benzo[*g,h,i*]perylene (BghiP). Nap, Acy, Ace, Flu, Phen and An are categorised as low molecular weight (LMW) PAHs with <4-ring structures, the remaining PAHs are categorised as high molecular weight (HMW) PAHs (≥4-rings) (Meador, 2008). Estimating risks to human health exclusively on the EPA16 creates uncertainty as the suite does not include other potentially more toxic compounds e.g. alkylated PAHs (Andersson and Achten, 2015).

The quantity and type of PAHs present in the environment initially depends on the source and the PAH formation process (Dong et al., 2012; Gao et al., 2016). A petrogenic source (crude oil and petroleum) synthesizes PAHs slowly under low temperatures, resulting in a high proportion of LMW PAHs and increased amounts of alkylated PAHs (Andersson and Achten, 2015). However, the petrogenic process of coalification can synthesize HMW PAHs, caused by aromatic ring condensation reactions. Consequently coals contain large and complex PAH compounds (Ribeiro et al., 2012; Mathews and Chaffee, 2012). Pyrogenic sources (coal carbonisation, vehicle exhaust, wildfires)

☆ This paper has been recommended for acceptance by Baoshan Xing.

* Corresponding author.
E-mail addresses: alelay@bgs.ac.uk (A.M. Williams-Clayson), darrenb@bgs.ac.uk (D.J. Beriro).

https://doi.org/10.1016/j.envpol.2023.122658
Received 27 June 2023; Received in revised form 11 September 2023; Accepted 28 September 2023
Available online 29 September 2023

alternatively form PAHs comparatively quickly by incomplete combustion of organic matter (OM) at high temperatures and result in abundant amounts of thermodynamically stable HMW parent PAHs (Kim et al., 2017; Ribeiro et al., 2012).

Sites where people could be exposed to soils with high PAH concentrations, e.g. formally contaminated sites under redevelopment, may require human health risk assessments (HHRAs) to evaluate the risks posed by the PAHs to human health and the actions required to address the risks (Gormley et al., 2011; Beriro et al., 2020). HHRAs use exposure models such as the Contaminated Land Exposure Assessment (CLEA) model to generate Generic Assessment Criteria (GAC) based on the exposure pathways, receptors, soil types, land use, contaminant concentrations, and toxicology (Cole and Jeffries, 2009). Numerous studies have reported that the quantity and type of soil OM is a dominant factor influencing the release and risk arising from PAHs from soil (Yu et al., 2018; Ehlers and Loibner, 2006). It is also known that the contribution of each exposure pathway towards the total human exposure will vary depending on the contaminant. LMW PAHs report a higher inhalation contribution percentage compared with HMW PAHs, due to the compound's physiochemical properties (e.g. volatility) (Nathanail et al., 2015). Thus, knowledge of the expected PAHs present at a site alongside soil properties can help assessors conducting HHRAs. Currently guidance on the BaP GAC for residential land use with plant uptake is 5 mg/kg. Soils above this are considered to pose a potentially unacceptable risk to human health (CL: AIRE, 2014).

Post-industrial sites commonly have soils with PAH concentrations above GAC values and thus pose potential risks to human health. A good example of such sites includes those which previously operated as Manufactured Gas Plants (MGPs), commonly known in the UK as gasworks. MGPs synthesised hydrogen and methane rich gas via the process of pyrolysis of coal or oil. MGPs produced a wide variety of wastes and by-products including scurf, ash, coal tar, coal, benzol, ammoniacal liquor, spent oxide, and foul lime (Thomas, 2014; Ruby et al., 2016). To improve the manufacturing efficiency, several MGP processes were developed. These include low temperature horizontal retorts (LTHR), high temperature horizontal retorts (HTHR), continuous vertical retorts (CVR), intermittent vertical coke ovens (IVCOs), coke ovens (COs), carburetted water gas (CWG), Tully plants (TP), heavy oil reforming plants (HORP), catalytic oil gas plants (COGP), and processes implemented to convert by-products to profitable goods such as tar distillation plants (TDP) and chemical plants (CP) (Gallacher et al., 2017b; Thomas, 2014).

The accuracy of HHRAs might be improved if the MGP process PAH distributions were known and targeted in assessments. Gallacher et al. (2017b), Thomas (2014) and McGregor et al. (2012) provide detailed descriptions of these MGP processes, such as the retort/chamber structures and pyrolysis temperatures used. They classified MGP processes by PAHs from end-member coal tars using two-dimensional gas chromatography (GC × GC) (McGregor et al., 2012; Gallacher et al., 2017b). In contrast our study investigates contaminated gasworks soils (GWS) using gas chromatography-mass spectrometry (GC-MS/MS), selected for its increased selectivity compared to full scan in GC-MS. This study also used a complementary screening technique called Rock-Eval (6) Pyrolysis (RE), initially used for oil exploration and more recently used to investigate different types of OM (Könitzer et al., 2016; Upton et al., 2018) and hydrocarbons in contaminated soils, predominately from oil spills (Lafargue et al., 1998). RE characterises the bulk OM by quantifying the release of hydrocarbons (detected by flame ionization) and the release of CO and CO_2 (monitored by infrared), recorded in response to the increasing temperature versus time throughout the pyrolysis and oxidation stages (Behar et al., 2001b; Lafargue et al., 1998). For our study RE was used to determine whether there were relationships between RE parameters, PAH distributions and MGP processes. To our knowledge only one other paper (Haeseler et al., 1999), measuring fewer samples and using an older RE technique (Rock-Eval III), has applied RE to GWS.

The research question for this study was whether GWS could be characterised by the MGP processes formally utilized at the site. Techniques to achieve this involved measuring 51 PAHs (30 parent and 21 alkylated) by GC-MS/MS and measuring bulk OM properties by RE. Using a combined approach allows for a enhanced understanding of the organic content of GWS. RE offers a rapid screening and a broader assessment of the overall organic compositions and GC-MS/MS provides detailed information on the PAH composition. We used the analytical data to explore relationships between RE parameters and PAH concentrations and distributions. In particular, we used the parent and alkylated PAH distributions, PAH diagnostic ratios, and principal component analysis (PCA). In summary, this research provides an understanding on identifying connections between MGP processes and the distributions of PAH contamination and OM fractions. These findings could inform which PAHs to target in risk estimation and management, helping to make HHRAs more accurate.

2. Materials and methodology

2.1. Sample collection and selection

A total of 93 soil samples were collected between 2016 and 2021 from 10 UK former MGP sites with periods of site inactivity ranging between 46 and 99 years, including a gasholder station, and a former tar distillation plant at a chemical works of a large city gasworks site. The locations of the sites are commercially sensitive and are not presented. Site and sample PAH and soil properties are detailed in both Tables 1 and SI Tables S1–2. Sample collection took place while the sites were under investigation or remediation by National Grid Property Holdings, which influenced where and when sampling could occur. Two background samples (BG) from local parks and a sub-set of 48 GWS (from the 93 collected GWS) were selected for PAH measurement using GC-MS/MS analysis. This sub-set was selected using stratified sampling and k-means clustering (k = 5) informed by RE analysis screening data.

2.2. Sample preparation

Directly after collection, soils were freeze-dried, disaggregated, and sieved through a 250 μm stainless steel mesh. Freeze drying minimises the effect of PAH losses from drying in comparison to other methods (Beriro et al., 2014). Subsequently, soils were stored in amber glass jars in a dark room in ambient conditions before sample preparation. ~1 g of the <250 μm fraction was spiked with 25 μg of deuterated PAH standards (surrogates used were phenanthrene-d10, pyrene-d10, benzo[*b*]fluoranthene-d12, benzo[*a*]pyrene-d12 and benzo[*g,h,i*]perylene-d12). PAHs from GWS were extracted by accelerated solvent extraction (ASE, Dionex-300) using DCM/acetone 1:1 v/v at a temperature of 100 °C and a pressure of 1500 psi. ASE extracts were diluted to 50 mL and a 400 μL aliquot was filtered by solid phase extraction (SPE) cartridges (Varian, Bond Elute TPH). The first SPE elution (1.5 mL of pentane) was discarded, the second elution containing PAHs was retained in 6 mL hexane/iso-propanol (96.6:3.4 v/v). Samples were blown down to 1 mL with a gentle stream of nitrogen before being spiked with 200 ng/mL of internal standards: fluorene-d10, fluoranthene-d10, perylene-d12 and indeno(1,2,3-cd)pyrene-d12. Further details of the spiking and extraction methods are presented in other papers (Vane et al., 2021; Vane et al., 2022).

2.3. PAH concentration

A total of 51 PAHs (PAH51) were quantified by GC-MS/MS; 30 parent PAHs (PAH30) and 21 grouped alkylated PAHs (Alkyl21) (SI: Tables S3 and S6). PAH concentrations were determined by Thermo Scientific Trace 1300 GC coupled to a Thermo Scientific TSQ9000 triple quadrupole (GC-MS/MS) using the selected reaction monitoring (SRM) mode, equipped with an Agilent Select PAH column (30 m length x 0.25

mm diameter x 0.15 μm film thickness). A 1 μL aliquot of sample was injected in splitless mode using a split flow of 15 mL/min at 0.7 min with an injection temperature of 70 °C, which was held for 2 min, ramping at 10 °C/min to 180 °C and a final ramp of 4 °C/min to 350 °C. Helium was used as the carrier gas. The GC-MS/MS measurements on the alkylated PAH series were determined following Ghetu et al. (2021) and Sørensen et al. (2016).

Calibrations were performed using six calibration concentrations of PAH reference mixtures (PAH-Mix 9, PAH-Mix 45 and PAH-Mix 183, Dr. Ehrenstorfer), spiked with deuterated surrogates and internal standards. To determine instrument performance and background signals, standards were processed the same as GWS and inter-dispersed every 20 samples within the GC-MS/MS runs. The standards included the calibration samples of 200 pg/μL, procedural blanks of toluene and 1 g of the certified reference material (CRM) (NIST-1944: New York/New Jersey Waterway). Surrogate recoveries in all samples and standards were quantified to determine method efficiency and used for analyte concentration corrections (SI Section S1 and Table S4).

2.4. Rock-Eval (6) pyrolysis

GWS were analysed using a Rock-Eval (6) pyrolyzer (Vinci Technologies) to characterise OM (Behar et al., 2001a). Powdered dry samples (~30 mg) underwent the RE technique applied from Upton et al. (2018), the performance of the instrument was tested, by comparison to accepted values of Institute Français du Pétrole standards (IFP 160000, S/N1 5–081,840). Eighteen parameters were determined and defined by Cooper et al. (2019), Behar et al. (2001b), Waters et al. (2020) and include.

- S1 (HC mg/g)- quantity of thermo-vaporized free hydrocarbons released during pyrolysis heating up to 200 °C.
- S2 (HC mg/g) - quantity of hydrocarbons released from thermal cracking of mature OM during pyrolysis temperatures up to 650 °C.
- TpkS2 (°C) - true temperature value of the maximum yield of hydrocarbon released for the S2 peak.
- S3, S3′, S3CO, and S3′CO (mg CO_2/g or mg CO/g) – measure of CO and CO_2 produced during pyrolysis for organic and/or mineral source.
- TOC(%) – total organic carbon calculated from the sum of the carbon moieties (HC, CO, and CO_2).
- RC(%) – residual carbon composed of thermally resistant OM that remains after pyrolysis and is combusted in the oxidation stage, calculated by $\left(S4CO_2 \times \frac{12}{440}\right) + \left(S4CO \times \frac{12}{280}\right)$.
- PC(%) - pyrolyzable carbon yielded during the pyrolysis stage, calculated using $(S1 + S2) \times 0.083 + \left(S3CO_2 \times \frac{12}{440}\right) + \left(S3CO \times \frac{12}{280}\right)$.
- HI (mg HC/g TOC) – hydrogen index measures the extent of hydrogenation and provides indication of bound hydrocarbons released relative to TOC, calculated from $S2 \times 100/TOC$.
- OI (mg O_2/g TOC) – oxygen index corresponds to the released amounts of oxygen from CO and CO_2 relative to TOC, deduced from $S3 \times 100/TOC$.
- PI – production index, gives an indication of maturity of sample using the calculation $S1/(S1 + S2)$.

The thermal stability of OM in the GWS was determined by 1) deconvolution of temperature nodes of 200–340 °C (A1), 340–400 °C (A2), 400–460 °C (A3) and >460 °C (A4), 2) determination of the immature OM index (I-index) and the refractory OM index (R-index), $I - index = Log\,10\,((A1 + A2)/A3)$, and $R - index = ((A3 + A4)/100)$ (Brown et al., 2023; Garcin et al., 2022; Sebag et al., 2016).

2.5. Data evaluation and statistical analysis

Data evaluation and statistical analyses included principal component analysis (PCA), Shapiro-Wilk test, Levene's test, one-way ANOVA, Welch's ANOVA, and the post-hoc tests – Tukey HSD, Games-Howell and Pairwise Wilcoxon Rank Sum tests, were performed using R Statical Software (R Core Team, 2023) (SI: Section S3).

3. Results and discussion

3.1. Distributions and concentrations of PAHs

3.1.1. Total PAH concentrations and ring size contributions

A summary of MGP processes and resulting PAH concentrations for each site are shown in Table 1. PAH concentrations for each GWS are shown in SI Table S6. Overall, ∑PAH51 concentrations in the GWS range between 23 mg/kg to 29,500 mg/kg (median of 636 mg/kg) and ∑EPA16 range between 15 mg/kg to 23,400 mg/kg (median of 375 mg/kg), these ranges are similar to previous MGP investigations (Thavamani et al., 2012; Haeseler et al., 1999; Stout and Brey, 2019). In comparison, the BG soils recorded a ∑EPA16 mean concentration of 60 mg/kg, comparable to the London soils ∑EPA16 mean of 56 mg/kg reported by Vane et al. (2014).

Site A had the largest variation in PAH ring size distributions with high amounts of 2- and 3- ring PAHs compared to other sites, (SI Figure S1a-b). Sites B, C, E1 and I also exhibited higher contributions towards 2- and 3-ring PAHs compared to other sites. 2-ring PAHs showed several statistically significant differences ($p < 0.05$) between sites E2, F, G, and H vs sites A, C, E1, D, and I. In contrast, sites D, E2, F, G and H had the highest proportion of 5- and 6-ring PAHs. No significant differences between sites using one-way ANOVA were found for the 3- to 6-ring PAHs for the ∑EPA16 and ∑Alkyl21 log transformed concentrations (SI Section S3). The results indicate that sites associated with multiple processes including processes utilizing oil are positively related to higher proportions of LMW PAHs.

3.1.2. Parent and alkylated PAH distributions

Parent and alkylated PAH ratios (SI Table S8) identified sites A, B, and I with the highest proportions of alkylated PAHs (low ratios). Sites C, D, and E1 reported the widest and most varied range of parent/alkylated PAH ratios. Sites C and E1 used multiple processes, which can account for the spread of ratios. The highest PAH concentrations (SI Table S6) were for the HMW PAHs Fla, Phen, and Pyr which are generated by high temperature condensations of LMW PAHs (Thavamani et al., 2012). Sites C and E1 gave the highest PAH concentrations with similar PAH distributions (Phen > Fla > Pyr > An > BaA > Flu ~ Chry > BaP ~ BbF > BghiP) and observed higher contributions of anthracene than other sites as well as higher Flu contributions. Site D is documented operating the IVCO process only and recorded the next highest PAH concentrations which yielded similar median PAH distributions to sites E2 and G, (Fla > Pyr > Phen > BaA/Chry), sites E2 and G can both be associated to HTHR. The median PAH distribution order was identical for sites H and F (except for anthracene) with highest contributions from Fla > Pyr > BaA > Chry, which both operated the LTHR process.

PCA was used to investigate whether PAH distributions could characterise MGP processes. PCA was trialled on multiple data sets (SI Figures S6-S10), the most distinguishable clustering of MGP processes was achieved using the individual PAHs as relative contribution percentages towards the ∑PAH51 and removing GWS with ∑PAH51 concentrations <100 mg/kg. Fig. 1 shows an annotated overview of the main observations detected in the multiple PCAs. The predominant observation shows positive associations between parent and alkylated Nap derivatives for site A, site I also had high contributions but not to the same degree. GWS sampled in locations of known CWG contamination (A17 and B8) were found in close proximity, showing strong

Table 1
Overview of sites MGP processes and PAH concentrations.

Site	Background	A	B	C	D	E1	E2	F	G	H	I
Type of Site	Background Park	MGP site	MGP site	MGP site	MGP site	MGP site	Chemical works	MGP site	MGP site	MGP site	Gasholder station
HTHR	–	Yes	Yes	Yes	–	Yes	Yes	–	Yes	–	Yes
LTHR	–	–	–		–	–	–	Yes	Yes	Yes	–
VR	–	CVR	CVR	CVR	IVCO	CVR	CVR	–	–	–	CVR
CWG	–	Yes	Yes	TP	–	Yes	Yes	–	–	–	Yes
Other Process	–	COGP, PFD, RP, OGR	CP	HORP	–	TDP	TDP	–	–	–	–
Samples collected	2	16	9	7	8	6	9	1	9	20	8
GC-MS/MS sampled	2	16	3	4	3	4	4	1	2	8	4
∑EPA16 [mg/kg]	52–68 (60, 60)	15–5173 (264, 905)	20–1448 (57, 510)	419 - 16,669 (4,988, 6767)	375–2486 (1,928, 1596)	564–23,370 (5,299, 8633)	201–880 (356, 448)	135	76–163 (119, 119)	103–4195 (465, 1009)	61–921 (453, 472)
∑Alkyl21 [mg/kg]	28–29 (28, 28)	8–4207 (183, 732)	30–1327 (33, 463)	99–6867 (210, 2794	197–693 (621, 504)	259–5954 (1,315, 2211)	69–263 (101, 133)	53	22–31 (26, 26)	33–1411 (143, 342	32–1295 (638, 651)
∑PAH51 [mg/kg]	85–98 (91, 91)	23. – 10,015 (455, 1756)	51–2981 (96, 1042)	594–2517 (7,597, 10,239)	636–3638 (2,829, 2368)	887–29,544 (8,899, 12,057)	310–1285 (521, 659)	221	110–233 (173, 173)	155–6576 (709, 1607)	104–2106 (1,338, 1222)

HTHR = high temperature horizonal retort, LTHR = low temperature horizontal retort, CWG = carburetted water gas, VR = vertical retort, CVR = continuous vertical retort, IVCO = intermittent vertical chamber oven, CP = chemical plant, RP = reforming plant, COGP = catalytic oil gas plant, TP = Tully plant (VR + CWG), TDP = tar distillation plant, OGR = Onia-Geigy reformers, and HORP = heavy oil reforming plant. PAH concentrations in brackets are median and mean.

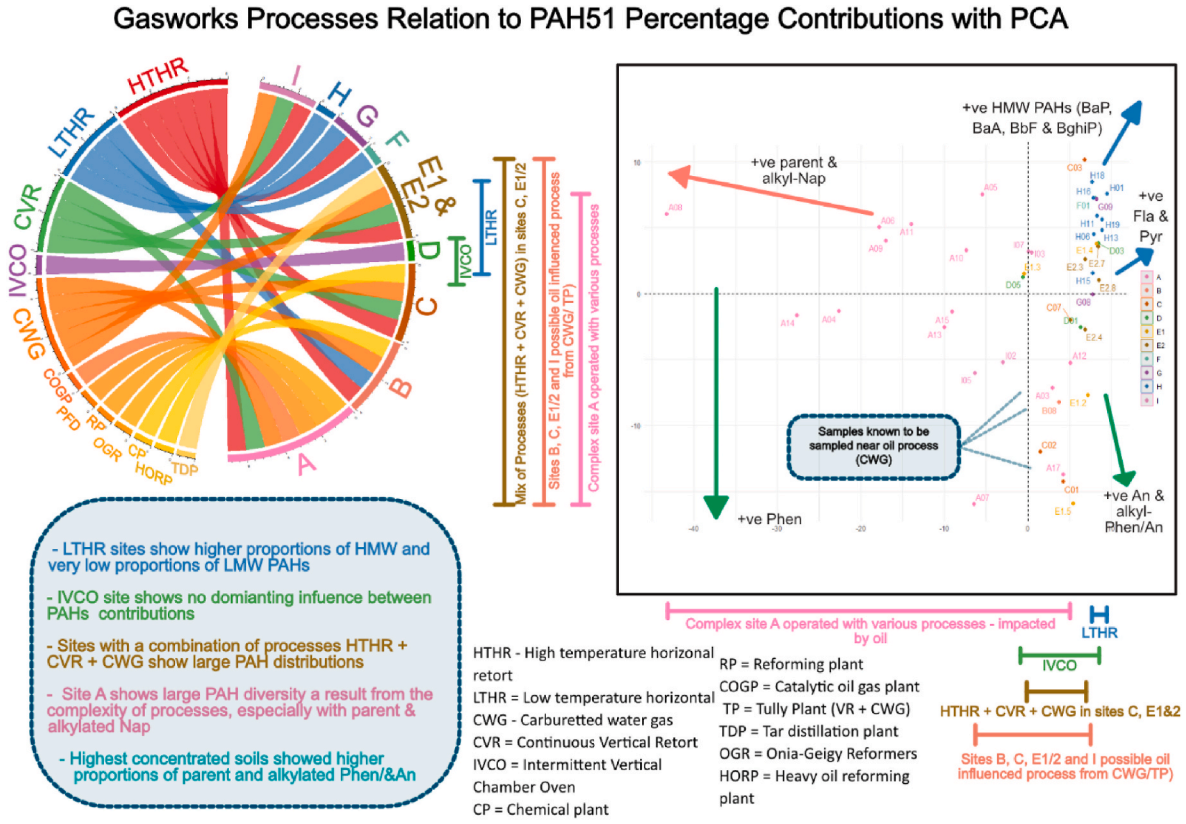

Fig. 1. Chord diagram to show the MGP processes related to each site and an annotated PCA biplot of GWS PAH percentage contributions towards ∑PAH51, GWS with ∑PAH51 < 100 mg/kg removed.

positive associations from Phen, Flu, and An and their alkylated derivatives, as were GWS reporting the highest PAH concentrations from sites C and E1. Indicating sites with CWG, HTHR and CVR processes are associated to higher contributions from the 3-ring PAH compounds.

GWS from sites associated with the LTHR process (sites F, G and H) showed positive associations towards the HMW PAHs (BaA, Chry, and BaP) and strong negative associations with LMW PAHs (Phen, Nap and Flu). GWS from the chemical works site E2 had slightly higher PC2 eigenvectors (weaker associations to Phen compounds) compared to the sites associated MGP site E1. Site D GWS populated near the origin of

both PC1 and PC2, indicating no dominating influence from individual PAHs associated with the IVCO process. Site C and E1 GWS in contrast varied by the PC2 eigenvector caused by differences with Phen compounds and HMW PAHs contributions, these sites have a range of processes including CVR, which would produce a diverse range of PAHs due to the process using a wide temperature gradient.

HHRAs typically concentrate on the EPA16 (Nathanail et al., 2015), in this study the EPA16 accounted for 32–79% of the total ∑PAH51%. Large proportions of alkylated PAHs were reported in the GWS, with the ∑Alkyl21 contributing between 7 and 65% to the total ∑PAH51%. This suggests that alkylated PAHs can be present in high proportions at MGP sites but are generally not accounted for in a HHRA, and thus HHRAs could be incorrectly estimating risks posed. The relative contribution of each alkylated series towards the ∑Alkyl21% between sites are in SI Figure S3. Generally, the alkylated series for alkyl-Flu and alkyl-DBT provide the lowest contributions, and the alkyl-Ph/An and alkyl-Fla/Pyr alkylated series provided the highest contributions. Conversely, sites A, B, and I (associated with CWG) differed to this trend by conferring the highest contribution from the alkyl-Nap series and lower contributions from the HMW alkylated-PAHs, presumed to be a result due to the CWG process typically using Gas Oil (similar to diesel). Sites F, G and H associated with LTHR processes in contrast observed the highest contributions from the HMW alkylated series alkyl-Ph/An > alkyl-Fla/Pyr > alkyl-BaA/Chry/TPh than other sites, with sites E1 and E2 displaying similar series distributions.

Alkylated PAH distribution signatures can assist in assigning PAH sources and were investigated for use in characterising MGP processes. An alkylated PAH homologue series with a "bell-shape" distribution signature is characterised as petrogenic, whereas a "slope-shape" following a decrease in concentration with an increase in the degree of alkylation is characterized as a pyrogenic source (Vane et al., 2021; Hindersmann and Achten, 2018). The slope of a pyrogenic alkylation distribution is dependent on the temperature, higher temperatures produce fewer alkylated PAHs creating a substantial decrease in the distribution slope (Stout et al., 2015). Examples of the alkylated PAH distributions for some of the GWS are shown in SI Figure S4. All GWS observed pyrogenic distributions for the alkylated series alkyl-Fla/Pyr and alkyl-BaA/Chry/TPh, and most GWS displayed pyrogenic distributions for alkyl-Ph/An except for samples A3, A7, and F1 which showed a petrogenic signature. The alkyl-DBT series displayed a petrogenic signature for all samples (except E1.2), a consequence of sulphur compounds associated with different oils (Douglas et al., 1996; McGregor et al., 2012). Distribution signatures were diverse within and between sites for the lower alkylated PAHs series alkyl-Nap and alkyl-Flu, potentially due to LMW PAHs being more susceptible to higher degrees of degradation compared to HMW PAHs, resulting in altered distribution signatures that differ from the original PAH source (Lima et al., 2005).

Consequently, the alkylated PAH distributions were unable to confidently characterise all MGP processes. However, they do show that the alkyl-Ph/An and alkyl-Fla/Pyr short chain alkylated compounds were the most predominant compounds from all the ∑Alkyl21 for GWS, apart from GWS highly influenced from oil processes reporting high alkyl-Nap compounds. Higher alkylation increases hydrophobicity and lowers vapour pressure (Achten and Andersson, 2015). This suggests that these heavier alkylated PAHs could potentially pose a greater risk through the human dermal and ingestion exposure pathways, compared to the inhalation which is driven by more volatile compounds. This study reports the widespread presence of alkylated PAHs in GWS, suggesting that a further understanding of their exposure and risk to humans from soil might form a focus in future HHRAs.

3.1.3. PAH diagnostic ratios

Contamination sources can be approximated by PAH diagnostic ratios which plot paired PAH isomer concentrations. The approach relies on the relative thermodynamic stabilities associated with different PAHs. Increased proportions of the less stable isomers are often found for parent PAHs formed at higher temperatures in combustion sources (Yunker et al., 2002; Vane et al., 2014). Twenty-one diagnostic ratios were explored in this study and several plotted into cross plots (SI: Table S8 and Figure S2a-k). These included thirteen diagnostic ratios which have been used previously by Ghetu et al. (2021) to identify sources of PAHs from CRMs. This study showed that most diagnostic ratios investigated were unable to distinguish GWS into related MGP processes. Generally, the ratios estimated pyrogenic/combustion sources, except for several GWS from sites A, B, and I linked to oil processes, which as might be expected often showed petrogenic ratio values.

The PAH diagnostic ratio cross plot which was the most useful at distinguishing processes was An/An + Phen vs Phen + An/(C0–C1-Ph/An) (SI Figure S2h) previously used by Pies et al. (2008). 32 GWS were in the combustion quadrant, and 16 GWS (from sites A, B, I and F) were in quadrants regarding petroleum influences. Sites H and F GWS (LTHR) displayed lower Phen + An/(C0–C1-Ph/An) ratios (0.44–0.62) than the other sites in the combustion quadrant suggesting lower C1-Phen/An proportions, however, site F is associated to a large degree of uncertainty due to the measurement on a single low concentrated GWS. Additionally, the cross-plot Fla + Pyr/(Fla + Pyr + C2–C4-Phen/An) vs (C1–C4-Phen/An)/Phen + An (SI Figure S2k) taken from Pies et al. (2008) showed GWS from site H with lower proportions of alkylated species (higher C1–C4-Phen/An)/Phen + An ratios) than the sites C, D, E1/2 and G. Whereas sites A, B, F and I GWS observed higher (C1–C4-Phen/An)/Phen + An ratios located in petrogenic zones. These cross-plot ratios suggest oil influenced processes can be associated with petrogenic ratio values and ratios involving alkylated species can differentiate LTHR processes from the other processes.

3.2. Rock-Eval (6) pyrolysis

3.2.1. S1 and S2

Twenty RE parameters were reported for the GWS (SI: Table S9), parameters S1 and S2 represent two hydrocarbon release stages at two temperature ranges during pyrolysis. S1 for the GWS ranged from not detected (ND) – 47.83 mg/g (median of 0.23 mg/g), with 69% of GWS being <1.00 mg/g. This shows that the bulk of GWS do not contain a large quantity of thermo-vaporized free hydrocarbons, S1 values are usually minor in soils as increased humification increases the degree of more complex hydrocarbons that typically require higher cracking temperatures (Disnar et al., 2003). Sites D, E2, F, G and H contained low S1 values. Sites A, B, C, E1 and I reported boarder S1 ranges (ND-47.83 mg/g) with higher S1 max values, this suggests that these sites were exposed to LMW organics, which corresponds to oil processes (Lafargue et al., 1998; Scheeder et al., 2020). GWS S2 values varied from 0.09 to 84.82 mg/g (median 6.02 mg/g), whereas Haeseler et al. (1999) reported GWS with a narrower ranges for both S2 (0.9–23.1 mg/g) and S1 values (0.2–14.2 mg/g), but both within this study's range. Hydrocarbons cracked in S2 are from natural and/or anthropogenic OM, which can have high PAH sorption capabilities depending on their abundance of macromolecular aliphatic chains, aromatic carbon components and quantities of flexible pores (Ukalska-Jaruga et al., 2019; Vane et al., 2022). The different S2 values in the GWS could be related to types of OM influencing the release of PAHs from soil.

The thermal stability of OM released in the pyrolysis cracking stages of the RE analysis can be explored using mathematical deconvolution of the S2 peak, either by calculating fractions using the base/tops of peaks or by focusing on peak areas in specified temperature ranges (Newell et al., 2016; Sebag et al., 2016; Ordoñez et al., 2019). Only Haeseler et al. (1999) has applied the deconvolution of S2 to GWS previously, but only into two fractions whereas recent studies use 4–5 temperature fractions. This study explored the selected temperature ranges specified by Sebag et al. (2016), Ordoñez et al. (2019), Malou et al. (2020) and Haeseler et al. (1999) (SI Figure S5). A positive correlation (R^2 = 0.6245) between the log transformed ∑PAH51 concentrations and the

lowest temperature range fraction percentage indicated that hydrocarbons cracked at these lower temperature ranges (A1) (Fig. 2b) included PAHs. Haeseler et al. (1999) concluded that the main constituents of the S1 and S2a peaks were aromatic hydrocarbons and resins, supporting this study's observations. Although no MGP processes were distinguished by deconvolution, GWS with the lowest PC2 values from PCA reported the highest A1 fraction percentages, implying that the extent of PAH contamination can be linked to the A1 fraction percentage. Future work exploring the relationship between a soils ability to release PAHs and the S2 deconvolution fractions has the prospect of relating rapid releasing PAH fractions with labile OM (James et al., 2016; Luthy et al., 1997) expressed by lower S2 temperature fractions.

The I-index and R-index calculated by the S2 deconvolution fractions can assess the preservation of thermally labile immature (readily decomposes) OM and the most persistent/refractory OM fractions (Sebag et al., 2016; Brown et al., 2023). The I/R diagram (Fig. 2d) shows GWS with the highest R-index originated from sites A, E2, G and H, however, the I/R diagram was unable to distinguish GWS by MGP process. The majority of GWS clustered at similar I-index values (−0.32-1.07) while the R-index spanned from 0.14 to 0.85. GWS with the highest concentrations observed the lowest R-index values and the highest I-index values. This suggests that GWS with higher concentrations contain high abundances of labile OM cracked at lower temperatures (e.g. LMW OM and aliphatics). Several GWS (in sites E2, G and H) had R-index (0.8–1.0) similar to coal reported by Sebag et al. (2016). These GWS can be assumed to have high amounts of immature geopolymers and/or refractory geopolymers, such as black carbon (BC), a source known to inhibit PAH release from soil (Luthy et al., 1997).

Overall, RE showed the pyrolyzed hydrocarbon fractions reporting oil impacted GWS with high S1, whereas S2 is more varied among GWS due to different combinations of OM types. Deconvolution of S2 showed PAHs released at lower temperatures (200–340 °C). Higher quantities of labile OM have been related to increased PAH desorption from soils compared to soils with higher proportions of recalcitrant/refractory OM (James et al., 2016; Lueking et al., 2000). Future research to enhance HHRAs could investigate using the R-index and S2 deconvolution to understand how likely PAHs may release from soils.

3.2.2. *Total organic carbon (TOC%), pyrolyzed carbon (PC%) and residual carbon (RC%)*

A wider range of TOC% was measured in this study (0.11–25.72%) compared to the study of US gasworks soils by Haeseler et al. (1999) (TOC% 1.82–10.14%). The PC% for this study was between 0.04 and 10.8% (mean 1.69%) and RC% between 0.07 and 23.3% (mean 6.6%), which couldn't be compared to Haeseler et al. (1999) as they did not report these parameters. Poot et al. (2014) discovered that

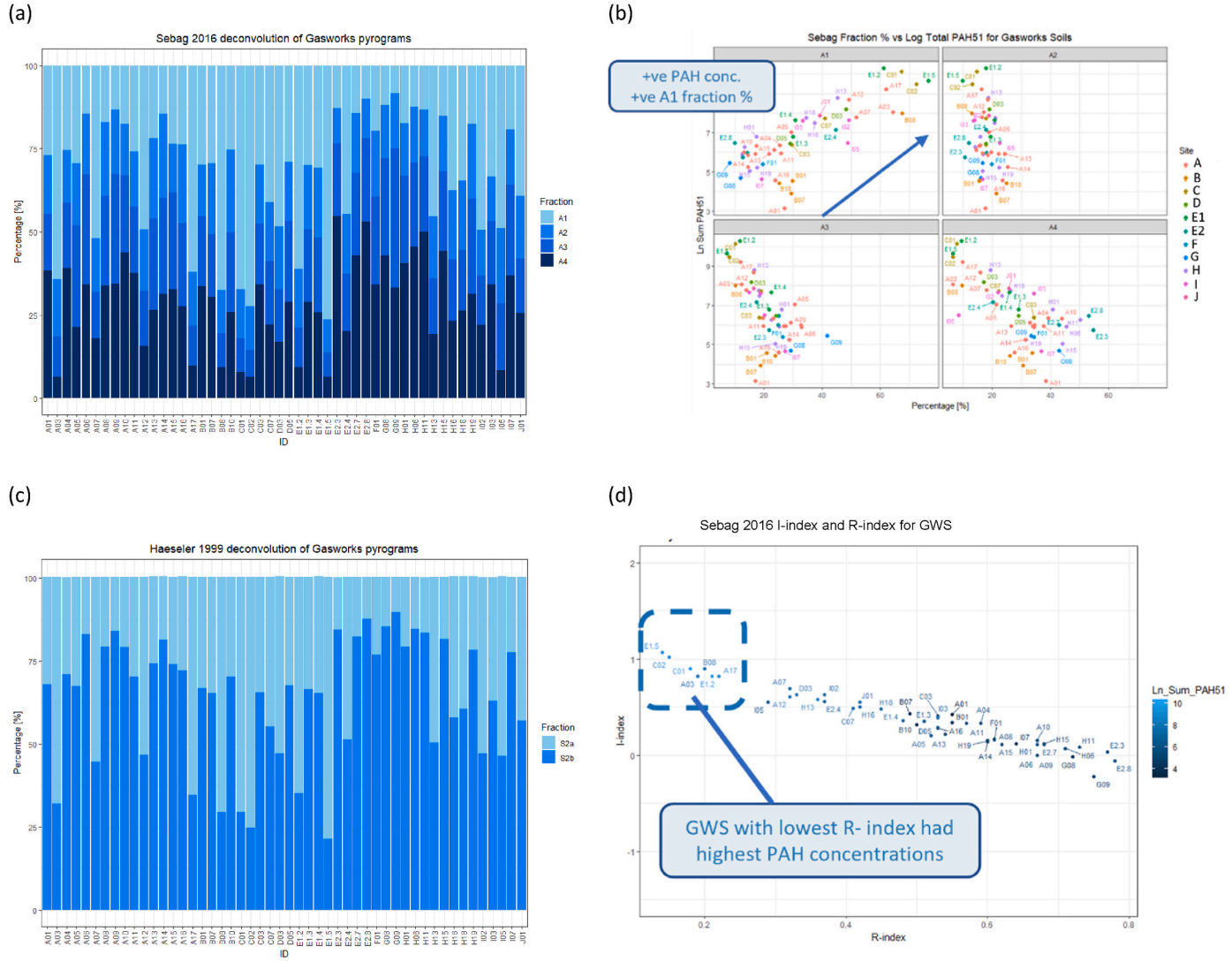

Fig. 2. S2 deconvolution fractions applied to GWS, (a) use of Sebag et al. (2016) fractions, (b) log PAH51 plotted against Sebag et al. (2016) fractions percentages, (c) use of Haeseler et al. (1999) fractions, (d) Sebag et al. (2016) I-index vs R-index plot created with 50/94 soils (soils with measured PAH concentrations).

approximately 7% of the RE RC% is BC, and that the RC% and BC correlations with PAH concentrations were associated with PAHs becoming trapped within the aromatic structure, hindering PAH release (Poot et al., 2014; Semple et al., 2013). Weak positive correlations were seen for this study's GWS TOC%, PC% and RC% against the log transformed total PAH concentrations. The PC% showed a broadly exponential increase for higher PAH concentrations than RC% and TOC%, an expected result given PAHs contribute towards lower temperature pyrolyzed fractions. Haeseler et al. (1999) also concluded that pyrolyzed hydrocarbons released ≤350 °C corresponded to 35–50% aromatic compounds. The PC%, RC% and TOC% for the background soils (means of 1.49%, 6.31%, and 7.80%) were within the ranges for the GWS, implying that without prior knowledge of the soil PAH concentrations these RE parameters would be unable to make assumptions about the soil's contamination history. However, the variation within these parameters suggests they have potential to be related to the ability of soil to capture/release PAHs.

3.2.3. Production index (PI), hydrogen index (HI), and oxygen index (OI)

Soil maturity can be estimated using PI, where PI < 0.1 is classed as immature (Waters et al., 2020). GWS PI ranged from ND-0.38 (mean of 0.08), GWS with the highest ∑PAH51 concentrations showed the highest PI values (SI Table S9). The HI measures the extent of hydrogenation. GWS provided a wide HI range between 8 and 549 mg/g where the highest HI values generally corresponded with the highest ∑PAH51 concentrations (e.g. the tar like materials A12 and E.12). A high HI suggests high contributions from hydrogen rich compounds such as long alkyl chains or alkyl-C and O-alkyl compounds, whereas a low HI indicates dehydrogenated and aromatic structures (BC and humic compounds) (Saenger et al., 2013). OI indicates the proportion of compounds containing oxygen, most GWS observed similar OI values < 100 mg/g (58% GWS), GWS with high OI values appear to have lower total PAH concentrations. Low OI for highly concentrated PAH GWS were expected given the elemental composition of coal tar is 5% oxygen and inorganics, compared to 86% carbon (Thomas, 2014).

Van Krevelen diagrams plots HI against OI and are widely used in oil exploration to classify the type of OM origin (Waters et al., 2020). The van Krevelen diagram (Fig. 3a) shows that GWS with lower OI have higher PAH concentrations. Specifically, a divide can be seen for GWS with HI > 200 mg/g reporting the highest ∑PAH51 concentrations,

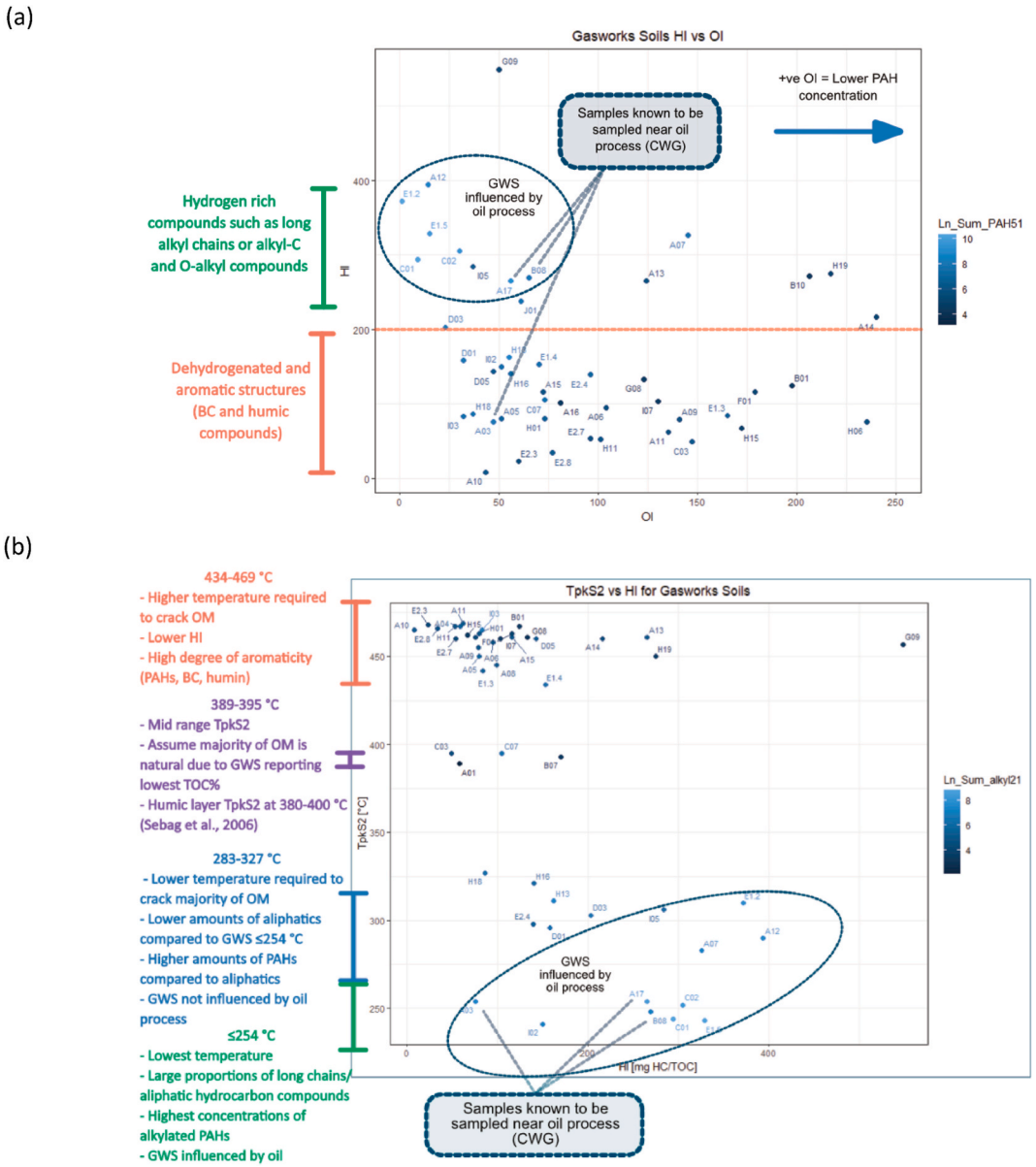

Fig. 3. (a) Annotated van Krevelen diagram (OI values above 250 have been removed), and (b) annotated TpkS2 vs HI plot.

although some samples in this range do not report high concentrations but have high HI values from natural OM, (e.g. one BG sample reported HI of 272 mg/g). Therefore, the van Krevelen diagram can help distinguish oil influenced processes (high HI) or non-oil influenced (low HI) when the PAH concentrations are known. GWS with HI > 200 mg/g were the same GWS reporting the strongest negative associations to PC2 in PCA and the highest A1 fraction percentages and were assumed to originate from a CWG petrogenic source. This contradicts the PAH ratios which suggested combustion origin for sites B, C and E1, indicating that the PAH ratios were unable to distinguish certain petrogenic identities found by the van Krevelen diagram.

3.2.4. TpkS2

The temperature at which the maximum amount of hydrocarbons released in S2 is described as the TpkS2. Higher TpkS2 temperatures indicate higher proportions of larger/stronger bound OM compounds in soils, GWS TpkS2 temperatures ranged from 241 to 480 °C. Different TpkS2 temperature range clusters were identified and plotted against the log transformed PAH concentrations and the HI shown in Fig. 3b. 35% of GWS had low TpkS2 temperatures between 241 and 327 °C, these GWS observed high log transformed PAH concentrations and high HI values. GWS with the lowest TpkS2 temperatures (≤254 °C) were obtained from sites (A, B, C, E1 and I) associated with oil, and observed the highest amounts of ∑Alkyl21 concentrations. This implies that GWS with lower TpkS2 temperatures compromise of large proportions of long chains/aliphatic hydrocarbon compounds that are thermally cracked at lower temperatures. Gallacher et al. (2017a) reported CWG tars with the highest relative concentrations of the *n*-alkanes, agreeing with this study that CWG/oil GWS will be dominated by aliphatic compounds compared to PAHs. GWS from sites D, E2 and H (not associated to oil processes) also reported low TpkS2 temperatures between 283 and 327 °C. However, these GWS had lower HI ≤ 203 mg/g, implying either lower amounts of aliphatics or the presence of higher amounts of PAHs compared to aliphatics. 56% of the GWS had a TpkS2 temperature between 434 and 469 °C and observed lower log transformed PAH concentrations and lower HI values than the GWS with lower TpkS2. This suggests that GWS with higher TpkS2 temperatures contain OM with a lower degree of hydrogenation and instead yield higher amounts of aromatic compounds such as PAHs, BC and natural macromolecular compounds that require higher cracking temperatures due to the quantity and strength of bonds. Although the lower PAH concentrations associated to the higher TpkS2 suggests influence from natural OM (Sebag et al., 2006). A low TpkS2 temperature therefore has the potential to relate to high PAH contamination from petrogenic sources containing higher amounts of aliphatic hydrocarbons (labile OM), potentially the TpkS2 could be used to predict PAH release from different soil OM fractions.

3.3. Characteristics of gasworks processes

Several methods were able to identify oil influenced and LTHR processes, whereas other processes were difficult to segregate from each other. The detailed results of these different analyses are described in SI Sections S4-8. Petrogenic characteristics were repeatedly reported for GWS from sites A, B, C, E1, E2 and I. These include high abundances of aliphatics, LMW PAHs, alkylated PAHs, and sulphur containing heterocycles (DBT compounds) compared to other processes (Gallacher et al., 2017b; McGregor et al., 2012). RE parameters showed high S1, low R-index values (≤0.22), and low TpkS2 temperatures linked to high HI values. Sites containing petrogenic origin PAHs can be related to the CWG and Tully plant processes, which operated at relatively low temperatures (650–700 °C) and sprayed oil to enrich the generated gas (Gallacher et al., 2017b; Thomas, 2014).

GWS associated with LTHR processes had higher distributions of HMW PAHs and lower proportions of LMW PAHs compared to other sites. Previous studies have reported higher levels of HMW PAHs associated with higher pyrolysis temperatures (Dong et al., 2012) and lower temperatures associated to LMW PAHs (Gao et al., 2016), due to the cracking of coal being the dominant reaction to PAHs formation. Potential reasons for our contrasting results include the potential that these sites had experienced greater degrees of weathering, particularly sites F and G which showed low PAH concentrations. Alternatively, both the low pyrolysis temperature and the coal type could influence the higher proportions of HMW PAHs (Dong et al., 2012; Yan et al., 2015; Gao et al., 2016). Pyrolysis of a high rank coal consisting of ≥4-ring PAHs (Yan et al., 2015), would generate HMW PAHs during pyrolysis. Han et al. (2020) reported higher emissions of HMW PAHs from lower temperatures in coal combustion, caused by the pyrolysis of the coal structure. However, Han et al. (2020) focused on combustion rather than pyrolysis.

This study did not investigate a site which solely operated with the HTHR or CVR process, which means making assumptions on these MGP processes is problematic. GWS associated with the HTHR and CVR tended to cluster together with pyrogenic characteristics. However, these GWS showed a great degree of variability for PAH distributions, which is expected due to the CVR temperature gradient generating products resembling characteristics of both low and high temperature processes (Gallacher et al., 2017b). Only site D operated solely under the IVCO process, IVCO used narrow, deep, and static chamber ovens to pyrolyze coal. The resulting IVCO products were very degraded, as seen in the PCA where no PAH species dominated the relative contributions. Additionally, differences between site E1 MGP and its associated chemical works plant site E2 were investigated and found that distillation released/decomposed LMW PAHs hence their lower abundance at Site E2.

3.4. Evaluation of applied methods

Previous studies (McGregor et al., 2012; Gallacher et al., 2017b) have succeeded in attributing MGP tars to a specific process. This study investigated soils and was not able to separate all MGP processes to the same degree. Reasons for this are likely to include not incorporating all compounds (e.g. alkanes) studied in the previous studies, potential weathering of samples affecting PAH distributions, impact of sample collection and site inactivity timespans, sites operating with multiple processes, and several soils being retrieved from mixed contamination sources. In addition, this study did not have access to end members (e.g. tars) to compare the soils to and at some sites there were only a small number of samples available with limited information on their provenance. However, these challenges can also be expected in real-world risk assessments where MGP sites might present serval unknowns due to missing information about the site history or sampling challenges. Despite the limitations identified this research provides novel insights into characteristics of different GWS from MGPs expected in real life scenarios using a carefully designed range analytical methods associated data evaluation tools.

This research observed several distinctive GWS characteristics linked to petrogenic oil processes and LHTR processes. Similar to McGregor et al. (2012), this study found PCA to be one of the best techniques to separate GWS based on MGP process, particularly between CWG and LTHR processes which observed contrasting distributions between LMW and HMW PAHs. The PAHs with the strongest influence in the PCA were Nap and Phen derivatives, Fla, Pyr and BaA, with Phen proportions influencing the MGP processes without oil application. RE parameters were able to strengthen the attribution for petrogenic contamination. However, the applied methods struggled to distinguish the IVCO, CVR and HTHR processes, for the reasons described.

PAH ratios using alkyl-Phen/An were able to characterise MGP processes influenced by oil and LTHR but were unable to characterise other processes, in contrast to McGregor et al. (2012) who were unable to distinguish processes using PAH diagnostic ratios on tars. The ratios used for this study were able to separate site H (LTHR) from the

predominant pyrogenic cluster, however, sites F and G were dissimilar to site H ratios (SI Figure S2h,k). These differences may have been caused by the small number of samples from site F and G which were unable to fully represent the LTHR, use of different coals, different weathering patterns, or other processes impacting GWS signatures. Although alkylated PAH distributions have been shown to be more reliable with source identification than PAH ratios (Hindersmann and Achten, 2018), GWS alkylated PAH distributions generally had similar results between MGP processes. LTHR sites were shown to have a higher degree of alkylated and parent HMW PAHs, although it is uncertain if weathering of LMW PAHs impacted this result.

RE parameters were unable to characterise MGP processes, however the RE parameters S1, TpkS2, HI, OI and the R-index used in conjunction with PAH concentrations and percentages provided insight into relationships between PAH contamination. This was particularly seen for processes with oil applications. GWS showed a large diversity in different RE parameters (e.g., S2, R-index), which showed potential for future work to relate these RE parameters with estimating the release of PAHs from soil OM fractions and the subsequent risk from PAHs. Other future work characterising GWS by MGP processes should include end members (specifically single process sites), investigate the impact of the time span of sample collection on PAH distributions and analyse greater numbers of GWS.

4. Conclusions

This research explores the characterisation of GWS by their retrospective MGP processes by: i) detailed evaluation of PAHs concentrations and their distributions of 30 parent and 21 alkylated PAHs quantified by GC-MS/MS; ii) characterisation of bulk organic matter properties using the relatively rapid evaluation method of RE. These methods facilitated the differentiation of GWS associated with oil contamination for CWG processes based on their distinctive PAH distributions (petrogenic origin) and reduced RE parameters (HI and TpkS2). While classifying other GWS based on MGP processes proved more challenging due to mixed contamination or limited samples, GWS associated to the LTHR process exhibited specific PAH profiles compared to other MGP processes.

PCA was able to characterise oil-contaminated and LTHR-associated GWS, aided by RE indices S1, TpkS2, HI, OI and the R-index. LMW PAHs predominated in oil related GWS, indicating an elevated inhalation exposure risk, while HMW PAHs were prominent in LTHR GWS, intensifying dermal and ingestion exposure concerns. Integration of PAH and bulk organic matter data suggests the potential for identifying GWS with labile organic matter fractions prone to higher PAH release and human health risks. This study supports risk assessment by informing the selection of critical PAHs linked to specific MGP processes. Importantly, alkylated PAHs emerged as process-dependent contributors to GWS, bearing heightened persistence and risk compared to parent PAHs. This research enhances understanding of PAH distributions and bulk organic matter fractions in former MGPs soils, facilitating more accurate risk assessment. By merging analytical techniques and data tools, it advances insights into PAH presence, distribution, and process-related risks.

Author statement

Conceptualization; Data curation; Formal analysis; Visualization; writing - original draft: AWC performed field work, all laboratory work, performed the measurements, analysed the data, and wrote the manuscript. Funding acquisition; Investigation; Methodology; Project administration: DJB was responsible for securing and management project funding. Methodology; Validation; Writing - review & editing: CHV, DB MJ, and RT supervised and provided feedback and helped shape the research project and manuscript. AK helped establish laboratory procedures and GC-MS/MS methods. CT provided site access for sampling and information regarding sites. All authors contributed to reviewing and editing the manuscript.

Declaration of competing interest

The authors declare that they have no known competing financial interests or personal relationships that could have appeared to influence the work reported in this paper.

Data availability

The data that has been used is confidential.

Acknowledgements

The authors gratefully acknowledge funding from the Natural Environment Research Council under the Envision DTP [NE/S007423/1], British Geological Survey [BUFI studentship S431] and industry funding from National Grid Property Holdings, UK [Contract reference GA_15F_147 WSP].

Appendix A. Supplementary data

Supplementary data to this article can be found online at https://doi.org/10.1016/j.envpol.2023.122658.

References

Achten, C., Andersson, J.T., 2015. Overview of polycyclic aromatic compounds (PAC). Polycycl. Aromat. Comp. 35, 177–186.
Andersson, J.T., Achten, C., 2015. Time to say goodbye to the 16 EPA PAHs? Toward an up-to-date use of PACs for environmental purposes. Polycycl. Aromat. Comp. 35, 330–354.
Behar, F., Beaumont, V., Penteado, D.B., 2001a. Rock eval 6 technology: perfomance and development. Oil Gas Sci. Technol. 56, 111–134.
Behar, F., Beaumont, V., Penteado, H.D.B., 2001b. Rock-Eval 6 technology: performances and developments. Oil Gas Sci. Technol. 56, 111–134.
Beriro, D.J., Cave, M., Kim, A., Craggs, J., Wragg, J., Thomas, R., Taylor, C., Nathanail, C. P., Vane, C., 2020. Soil-sebum partition coefficients for high molecular weight polycyclic aromatic hydrocarbons (HMW-PAH). J. Hazard Mater., 122633
Brown, C., Boyd, D.S., Sjögersten, S., Vane, C.H., 2023. Detecting tropical peatland degradation: combining remote sensing and organic geochemistry. PLoS One 18, e0280187.
CL: AIRE, 2014. SP1010 – development of category 4 screening levels for assessment of land affected by contamination. Department for Environment Food and Rural Affairs: Contaminated Land: Applications in Real Environments.1, pp. 1–18.
Cole, S., Jeffries, J., 2009. Using Soil Guideline Values. Bristol.
Cooper, H.V., Vane, C.H., Evers, S., Aplin, P., Girkin, N.T., Sjögersten, S., 2019. From peat swamp forest to oil palm plantations: the stability of tropical peatland carbon. Geoderma 342, 109–117.
Disnar, J.R., Guillet, B., Keravis, D., DI-Giovanni, C., Sebag, D., 2003. Soil organic matter (SOM) characterization by Rock-Eval pyrolysis: scope and limitations. Org. Geochem. 34, 327–343.
Dong, J., Li, F., Xie, K., 2012. Study on the source of polycyclic aromatic hydrocarbons (PAHs) during coal pyrolysis by PY–GC–MS. J. Hazard Mater. 243, 80–85.
Douglas, G.S., Bence, A.E., Prince, R.C., Mcmillen, S.J., Butler, E.L., 1996. Environmental stability of selected petroleum hydrocarbon source and weathering ratios. Environ. Sci. Technol. 30, 2332–2339.
Ehlers, G.A.C., Loibner, A.P., 2006. Linking organic pollutant (bio)availability with geosorbent properties and biomimetic methodology: a review of geosorbent characterisation and (bio)availability prediction. Environ. Pollut. 141, 494–512.
Gallacher, C., Thomas, R., Lord, R., Kalin, R.M., Taylor, C., 2017a. Comprehensive database of manufactured gas plant tars–Part B aliphatic and aromatic compounds. Rapid Commun. Mass Spectrom. 31, 1239–1249.
Gallacher, C., Thomas, R., Lord, R., Kalin, R.M., Taylor, C., 2017b. Comprehensive database of manufactured gas plant tars. Part A. Database. Rapid Commun. Mass Spectrom. 31, 1231–1238.
Gao, M., Wang, Y., Dong, J., Li, F., Xie, K., 2016. Release behavior and formation mechanism of polycyclic aromatic hydrocarbons during coal pyrolysis. Chemosphere 158, 1–8.
Garcin, Y., Schefuß, E., Dargie, G.C., Hawthorne, D., Lawson, I.T., Sebag, D., Biddulph, G. E., Crezee, B., Bocko, Y.E., Ifo, S.A., Mampouya Wenina, Y.E., Mbemba, M., Ewango, C.E.N., Emba, O., Bola, P., Kanyama Tabu, J., Tyrrell, G., Young, D.M., Gassier, G., Girkin, N.T., Vane, C.H., Adatte, T., Baird, A.J., Boom, A., Gulliver, P., Morris, P.J., Page, S.E., Sjögersten, S., Lewis, S.L., 2022. Hydroclimatic vulnerability of peat carbon in the central Congo Basin. Nature. 612, 277–282.
Ghetu, C.C., Scott, R.P., Wilson, G., Liu-May, R., Anderson, K.A., 2021. Improvements in identification and quantitation of alkylated PAHs and forensic ratio sourcing. Anal. Bioanal. Chem.. 413, 1651–1664.

Gormley, A., Pollard, S., Rocks, S., 2011. Guidelines for environmental risk assessment and management: green Leaves III, 1. Cranfiled University, Department for Environmental Food and Rural Affairs, pp. 1–82.
Haeseler, F., Blanchet, D., Druelle, V., Werner, P., Vandecasteele, J.-P., 1999. Analytical characterization of contaminated soils from former manufactured gas plants. Environ. Sci. Technol. 33, 825–830.
Han, Y., Chen, Y., Feng, Y., Song, W., Cao, F., Zhang, Y., Li, Q., Yang, X., Chen, J., 2020. Different formation mechanisms of PAH during wood and coal combustion under different temperatures. Atmos. Environ. 222, 117084.
Hindersmann, B., Achten, C., 2018. Urban soils impacted by tailings from coal mining: PAH source identification by 59 PAHs, BPCA and alkylated PAHs. Environ. Pollut. 242, 1217–1225.
International Agency For Research On Cancer, 2010. *Some non-Heterocyclic Polycyclic Aromatic Hydrocarbons and Some Related Exposures,* World Health Organisation. IARC Press, International Agency for Research on Cancer, Lyon, France.
James, K., Peters, R.E., Cave, M.R., Wickstrom, M., Lamb, E.G., Siciliano, S.D., 2016. Predicting polycyclic aromatic hydrocarbon bioavailability to mammals from incidentally ingested soils using partitioning and fugacity. Environ. Sci. Technol. 50, 1338–1346.
Kim, A.W., Vane, C.H., Moss-Hayes, V.L., Beriro, D.J., Nathanail, C.P., Fordyce, F.M., Everett, P.A., 2017. Polycyclic aromatic hydrocarbons (PAHs) and polychlorinated biphenyls (PCBs) in urban soils of Glasgow, UK. Earth and Environmental Science Transactions of the Royal Society of Edinburgh 108, 231–247.
Könitzer, S.F., Stephenson, M.H., Davies, S.J., Vane, C.H., Leng, M.J., 2016. Significance of sedimentary organic matter input for shale gas generation potential of Mississippian Mudstones, Widmerpool Gulf, UK. Rev. Palaeobot. Palynol. 224, 146–168.
Lafargue, E., Marquis, F., Pillot, D., 1998. Rock-Eval 6 applications in hydrocarbon exploration, production, and soil contamination studies. Rev. Inst. Fr. Petrol 53, 421–437.
Lima, A.L.C., Farrington, J.W., Reddy, C.M., 2005. Combustion-derived polycyclic aromatic hydrocarbons in the environment—a review. Environ. Forensics 6, 109–131.
Lueking, A.D., Huang, W., Soderstrom-Schwarz, S., Kim, M., Weber, W.J., 2000. Relationship of soil organic matter characteristics to organic contaminant sequestration and bioavailability. J. Environ. Qual. 29, 317–323.
Luthy, R.G., Aiken, G.R., Brusseau, M.L., Cunningham, S.D., Gschwend, P.M., Pignatello, J.J., Reinhard, M., Traina, S.J., Weber, W.J., Westall, J.C., 1997. Sequestration of hydrophobic organic contaminants by geosorbents. Environ. Sci. Technol. 31, 3341–3347.
Malou, O.P., Sebag, D., Moulin, P., Chevallier, T., Badiane-Ndour, N.Y., Thiam, A., Chapuis-Lardy, L., 2020. The Rock-Eval® signature of soil organic carbon in arenosols of the Senegalese groundnut basin. How do agricultural practices matter? Agric. Ecosyst. Environ. 301, 107030.
Mathews, J.P., Chaffee, A.L., 2012. The molecular representations of coal – a review. Fuel 96, 1–14.
Mcgregor, L.A., Gauchotte-Lindsay, C., Nic Daéid, N., Thomas, R., Kalin, R.M., 2012. Multivariate statistical methods for the environmental forensic classification of coal tars from former manufactured gas plants. Environ. Sci. Technol. 46, 3744–3752.
Meador, J., 2008. Polycyclic aromatic hydrocarbons. In: JØRGENSEN, S.E., FATH, B.D. (Eds.), Encyclopedia of Ecology. Academic Press, Oxford.
Nathanail, C.P., Mccaffrey, C., Gillett, A.G., Ogden, R.C., Nathanail, J.F., 2015. *The LQM/CIEH S4ULs for Human Health Risk Assessment,* Nottingham. Land Quality Press, Nottingham.
Newell, A.J., Vane, C.H., Sorensen, J.P., Moss-Hayes, V., Gooddy, D.C., 2016. Long-term Holocene groundwater fluctuations in a chalk catchment: evidence from Rock-Eval pyrolysis of riparian peats. Hydrol. Process. 30, 4556–4567.
Ordoñez, L., Vogel, H., Sebag, D., Ariztegui, D., Adatte, T., Russell, J.M., Kallmeyer, J., Vuillemin, A., Friese, A., Crowe, S.A., Bauer, K.W., Simister, R., Henny, C., Nomosatryo, S., Bijaksana, S., 2019. Empowering conventional Rock-Eval pyrolysis for organic matter characterization of the siderite-rich sediments of Lake Towuti (Indonesia) using End-Member Analysis. Org. Geochem. 134, 32–44.
Pies, C., Hoffmann, B., Petrowsky, J., Yang, Y., Ternes, T.A., Hofmann, T., 2008. Characterization and source identification of polycyclic aromatic hydrocarbons (PAHs) in river bank soils. Chemosphere 72, 1594–1601.
Poot, A., Jonker, M.T.O., Gillissen, F., Koelmans, A.A., 2014. Explaining PAH desorption from sediments using Rock Eval analysis. Environ. Pollut. 193, 247–253.
R CORE TEAM, 2023. R: A Language and Environment for Statistical Computing. R Foundation for Statistical Computing, Vienna, Austria.
Ribeiro, J., Silva, T., Filho, J.G.M., Flores, D., 2012. Polycyclic aromatic hydrocarbons (PAHs) in burning and non-burning coal waste piles. J. Hazard Mater. 199–200, 105–110.
Ruby, M.V., Lowney, Y.W., Bunge, A.L., Roberts, S.M., Gomez-Eyles, J.L., Ghosh, U., Kissel, J.C., Tomlinson, P., Menzie, C., 2016. Oral bioavailability, bioaccessibility, and dermal absorption of PAHs from soil—state of the science. Environ. Sci. Technol. 50, 2151–2164.
Saenger, A., Cécillon, L., Sebag, D., Brun, J.-J., 2013. Soil organic carbon quantity, chemistry and thermal stability in a mountainous landscape: a Rock–Eval pyrolysis survey. Org. Geochem. 54, 101–114.
Scheeder, G., Weniger, P., Blumenberg, M., 2020. Geochemical implications from direct Rock-Eval pyrolysis of petroleum. Org. Geochem. 146, 104051.
Sebag, D., Disnar, J.-R., Guillet, B., DI Giovanni, C., Verrecchia, E.P., Durand, A., 2006. Monitoring organic matter dynamics in soil profiles by 'Rock-Eval pyrolysis': bulk characterization and quantification of degradation. Eur. J. Soil Sci. 57, 344–355.
Sebag, D., Verrecchia, E.P., Cécillon, L., Adatte, T., Albrecht, R., Aubert, M., Bureau, F., Cailleau, G., Copard, Y., Decaens, T., Disnar, J.R., Hetényi, M., Nyilas, T., Trombino, L., 2016. Dynamics of soil organic matter based on new Rock-Eval indices. Geoderma 284, 185–203.
Semple, K.T., Riding, M.J., Mcallister, L.E., Sopena-Vazquez, F., Bending, G.D., 2013. Impact of black carbon on the bioaccessibility of organic contaminants in soil. J. Hazard Mater. 261, 808–816.
Sørensen, L., Meier, S., Mjøs, S.A., 2016. Application of gas chromatography/tandem mass spectrometry to determine a wide range of petrogenic alkylated polycyclic aromatic hydrocarbons in biotic samples. Rapid Commun. Mass Spectrom. 30, 2052–2058.
Stout, S.A., Brey, A.P., 2019. Appraisal of coal- and coke-derived wastes in soils near a former manufactured gas plant, Jacksonville, Florida. Int. J. Coal Geol. 213, 103265.
Stout, S.A., Emsbo-Mattingly, S.D., Douglas, G.S., Uhler, A.D., Mccarthy, K.J., 2015. Beyond 16 priority pollutant PAHs: a review of PACs used in environmental forensic chemistry. Polycycl. Aromat. Comp. 35, 285–315.
Thavamani, P., Megharaj, M., Naidu, R., 2012. Multivariate analysis of mixed contaminants (PAHs and heavy metals) at manufactured gas plant site soils. Environ. Monit. Assess. 184, 3875–3885.
Thomas, R., 2014. Gasworks profile A: the history and operation of gasworks (manufactured gas plants) in britain. Contaminated Land: Applications in Real Environments (CL: AIRE), London. London WC1B 3QJ: Contaminated Land: Applications in Real Environments (CL:AIRE) 1, 1–50.
Ukalska-Jaruga, A., Smreczak, B., Klimkowicz-Pawlas, A., 2019. Soil organic matter composition as a factor affecting the accumulation of polycyclic aromatic hydrocarbons. J. Soils Sediments 19, 1890–1900.
Upton, A., Vane, C.H., Girkin, N., Turner, B.L., Sjögersten, S., 2018. Does litter input determine carbon storage and peat organic chemistry in tropical peatlands? Geoderma 326, 76–87.
Vane, C., Kim, A., Beriro, D., Cave, M., Lowe, S., Lopes Dos Santos, R., Ferreira, A., Collins, C., 2021. Persistent organic pollutants in urban soils of central London, england, UK: measurement and spatial modelling of black carbon (BC), petroleum hydrocarbons (TPH), polycyclic aromatic hydrocarbons (PAH) and polychlorinated biphenyls (PCB). Adv. Environ. Eng. Res. 2, 012.
Vane, C.H., Kim, A.W., Beriro, D.J., Cave, M.R., Knights, K., Moss-Hayes, V., Nathanail, P.C., 2014. Polycyclic aromatic hydrocarbons (PAH) and polychlorinated biphenyls (PCB) in urban soils of Greater London, UK. Appl. Geochem. 51, 303–314.
Vane, C.H., Kim, A.W., Lopes Dos Santos, R.A., Gill, J.C., Moss-Hayes, V., Mulu, J.K., Mackie, J.R., Ferreira, A.M.P.J., Chenery, S.R., Olaka, L.A., 2022. Impact of organic pollutants from urban slum informal settlements on sustainable development goals and river sediment quality, Nairobi, Kenya, Africa. Appl. Geochem. 146, 105468.
Waters, C.N., Vane, C.H., Kemp, S.J., Haslam, R.B., Hough, E., Moss-Hayes, V.L., 2020. Lithological and chemostratigraphic discrimination of facies within the bowland shale formation within the craven and edale basins, UK. Petrol. Geosci. 26, 325–345.
Yan, L., Bai, Y., Zhao, R., Li, F., Xie, K., 2015. Correlation between coal structure and release of the two organic compounds during pyrolysis. Fuel 145, 12–17.
Yu, L., Duan, L., Naidu, R., Semple, K.T., 2018. Abiotic factors controlling bioavailability and bioaccessibility of polycyclic aromatic hydrocarbons in soil: putting together a bigger picture. Sci. Total Environ. 613–614, 1140–1153.
Yunker, M.B., Macdonald, R.W., Vingarzan, R., Mitchell, R.H., Goyette, D., Sylvestre, S., 2002. PAHs in the Fraser River basin: a critical appraisal of PAH ratios as indicators of PAH source and composition. Org. Geochem. 33, 489–515.